

EVOLUTION OF 3–9 M_{\odot} STARS FOR $Z = 0.001$ – 0.03 AND METALLICITY EFFECTS ON TYPE Ia SUPERNOVAE

HIDEYUKI UMEDA AND KEN'ICHI NOMOTO

Research Center for the Early Universe and Department of Astronomy, School of Science, University of Tokyo, Bunkyo-ku, Tokyo 113-0033, Japan; umeda@iron.astron.s.u-tokyo.ac.jp, nomoto@astron.s.u-tokyo.ac.jp

HITOSHI YAMAOKA

Department of Physics, Faculty of Science, Kyushu University, Ropponmatsu, Fukuoka 810-8560, Japan; yamaoka@rc.kyushu-u.ac.jp

AND

SHINYA WANAJO

Division of Theoretical Astrophysics, National Astronomical Observatory, Mitaka, Tokyo 181-8588, Japan; wanajo@diamond.mtk.nao.ac.jp

Received 1998 June 25; accepted 1998 October 6

ABSTRACT

Recent observations have revealed that Type Ia supernovae (SNe Ia) are not perfect standard candles; they show variations in their absolute magnitudes, light-curve shapes, and spectra. The C/O ratio in the SNe Ia progenitors (C-O white dwarfs) may be related to this variation. In this work, we systematically investigate the effects of stellar mass (M) and metallicity (Z) on the C/O ratio and its distribution in the C-O white dwarfs by calculating stellar evolution from the main sequence through the end of the second dredge-up for $M = 3$ – $9 M_{\odot}$ and $Z = 0.001$ – 0.03 . We find that the total carbon mass fraction just before SN Ia explosion varies in the range 0.36–0.5. We also calculate the metallicity dependence of the main-sequence mass range of the SN Ia progenitor white dwarfs. Our results show that the maximum main-sequence mass to form C-O white dwarfs decreases significantly toward lower metallicity, and the number of SN Ia progenitors may be underestimated if metallicity effect is neglected. We discuss the implications of these results on the variation of SNe Ia, determination of cosmological parameters, luminosity function of white dwarfs, and galactic chemical evolution.

Subject headings: nuclear reactions, nucleosynthesis, abundances — stars: abundances — stars: evolution — stars: interiors — supernovae: general — white dwarfs

1. INTRODUCTION

Type Ia supernovae (SNe Ia) are characterized by the absence of hydrogen and the presence of a strong Si II line in the early time spectra. The majority of SNe Ia have almost the same absolute brightness, thereby being good distance indicators for determining cosmological parameters (e.g., Branch & Tammann 1992; Sandage & Tammann 1993; see Nomoto, Iwamoto, & Kishimoto 1997 for a recent review). However, SNe Ia are not perfect standard candles; they show some variations in their absolute magnitudes, light-curve shapes, and spectra (Phillips 1993; Branch, Romanishin, & Baron 1996; Hamuy et al. 1996). It is important to understand the source of these variations and their dependence on metallicity in order to use high-redshift SNe Ia for determining cosmological parameters.

It is widely accepted that SNe Ia are thermonuclear explosions of accreting C-O white dwarfs (WDs), although the details of the explosion mechanism are still under debate (e.g., Ruiz-Lapuente, Canal, & Isern 1997). Previous studies have shown that typical SNe Ia are well described by the Chandrasekhar mass model, in which accreting C-O WDs explode when their masses approach the critical mass $M_{\text{Ia}} \simeq 1.37$ – $1.38 M_{\odot}$ (Nomoto, Thielemann, & Yokoi 1984; Höflich & Khokhlov 1996). The explosion is induced by carbon ignition in the central region and subsequent propagation of the burning front. Behind the burning front, explosive burning produces a large amount of ^{56}Ni . There are two models for the burning front propagation: the deflagration model (e.g., Nomoto, Sugimoto, & Neo 1976; Nomoto et al. 1984) and the delayed (or late) detonation (DD) model (Khokhlov 1991; Yamaoka et al. 1992; Woosley & Weaver 1994).

There are several possible sources of the variations of brightness and spectra: for example, variations of the age and mass accretion rates of the WDs, which affect the ignition density; variations of the WD progenitor's main-sequence mass and metallicity, which affect the C/O ratio in the WDs; and variation of the deflagration-detonation transition density (ρ_{tr}) in the DD model. These variations modify the explosion energy and the synthesized ^{56}Ni mass, which in turn affect the maximum brightness and shape of the SN Ia light curve.

Previous explosion models have assumed a uniform mass fraction ratio $C/O = 1$, although previous results indicated that $C/O < 1$ in the central region (e.g., Mazzitelli & D'Antona 1986a, 1986b; Schaller et al. 1992, hereafter SSMM). This was partly for simplicity and partly because of the C/O ratio's strong sensitivity to the treatment of convection and the $^{12}\text{C}(\alpha, \gamma)^{16}\text{O}$ rate. However, the effect of the different C/O ratio is not negligible. For example, Höflich, Wheeler, & Thielemann (1998) recently constructed explosion models by arbitrarily changing the C/O ratio to $C/O = \frac{2}{3}$ and found some significant effects on the light curve and spectra.

Intermediate-mass stars by definition burn only hydrogen and helium, and they form C-O cores after He burning. These cores will become C-O WDs, thus becoming SNe Ia progenitors in certain binary systems. Previously, several groups have investigated intermediate-mass stars, but they have not paid much attention to the C/O ratio and the C-O core mass size and its systematic dependence on the stellar mass and metallicity, as well as its effects on SNe Ia. For example, SSMM and a series of subsequent papers (Schaerer et al. 1993; Charbonnel et al. 1993) studied the

influence of the metallicity on the lifetimes, luminosities, and chemical structure of intermediate-mass stars. However, they showed only the central and surface chemical abundances; they did not show the C-O core mass sizes. Salaris et al. (1997) showed the radial profile of the C/O ratio of intermediate-mass stars as well as the C-O core mass size, but only for solar metallicity. Vassiliadis & Wood (1993) calculated C-O core mass sizes for the stars below $5 M_{\odot}$ but did not pay much attention to the C/O ratio. Works prior to 1992, such as Castellani, Chieffi, & Straniero (1990), Tornambè & Chieffi (1986), and Becker & Iben (1979), used Los Alamos (Huebner et al. 1977) or Cox & Stewart (1970) opacity tables, and their results would be significantly different if the latest OPAL opacity (Iglesias & Rogers 1993) were used.

In this paper, using updated input physics, we evolve the intermediate-mass ($3\text{--}9 M_{\odot}$) stars and examine the stellar metallicity and mass dependence of the C/O ratio, its radial profile, and the C-O core mass size. These quantities are sensitive to the treatment of convective mixing; however, for the same treatment of convection, these are dominantly determined by the $^{12}\text{C}(\alpha, \gamma)^{16}\text{O}$ rate. As described in § 2, we calibrate this rate by the massive star nucleosynthesis.

We also obtain the metallicity dependence of zero-age main-sequence (ZAMS) mass ranges of SN Ia progenitors, and especially its upper limit M_{UP} , where M_{UP} is the ZAMS mass at the border between stars that ignite carbon under nondegenerate conditions and stars that form a strong degenerate C-O core. This quantity has various important applications for the determination of, for example, galactic chemical evolution and the luminosity function of WDs in our Galaxy. However, earlier determination of M_{UP} was based on old radiative opacity tables (e.g., Becker & Iben 1979, hereafter BI79; Castellani et al. 1985, hereafter CCPT; Tornambè & Chieffi 1986; Castellani et al. 1990) or inexact calculations (Schaerer et al. 1993). Moreover, calculations made during the 1980s and early 1990s often assumed strong overshooting or breathing pulses, which may not be desirable with the use of the OPAL opacity. The results are qualitatively consistent with ours but quantitatively different. Our M_{UP} is significantly smaller than the estimates in BI79 for all Z we calculated, and smaller for that found in Schaefer et al. (1993) for $Z \lesssim 0.01$. It also shows a large decrease toward lower metallicity. Such a dependence would be important for the distributions of SNe Ia brightness as a function of metallicity.

This paper is organized as follows. In the next section, our numerical code, input physics, and parameters are described. Section 3 shows our results and compares them with those of previous works. Their implications are discussed in § 4.

2. NUMERICAL CODE AND ASSUMPTIONS

We modify and update the Henyey type stellar evolution code (Saio & Nomoto 1988). Important improvements include the use of the OPAL radiative opacity (Iglesias & Rogers 1993), neutrino emissivity (Itoh, Nishikawa, & Kohyama 1996), and a nuclear reaction network with a larger number of isotopes. Most of the nuclear reaction rates are provided by Thielemann (1995, private communication). This network is coupled to the dynamical equations for stellar evolution in a manner *implicitly* similar to SSMM and Weaver & Woosley (1993). That is, the network, with a reduced number of isotopes, is run during

Henyey relaxation. Nuclear energy generation rates between the reduced and full networks are almost identical. After dynamics is converged, nucleosynthesis is calculated with a full network code for He burning. The isotopes included are shown in Table 1. For H burning, the network code of Saio & Nomoto (1988) is used with updated nuclear reaction rates.

Treatment of convection is one of the serious uncertainties in the theory of stellar evolution. We adopt the Schwarzschild criterion for convective instability and the diffusive treatment for the convective mixing (Spruit 1992; Saio & Nomoto 1998). This formalism contains a parameter f_k of order unity that is proportional to the diffusion coefficient and also to the square root of the ratio of “solute” to thermal diffusivity. We found that the results were not sensitive to this parameter, at least in the range $f_k \simeq 0.1\text{--}1$. In this paper, we set $f_k = 0.3$. We use the mixing-length parameter $\alpha = 1.5$ for the outermost superadiabatic convection. Chieffi, Straniero, & Salaris (1995) found that a larger value ($\alpha \simeq 2.25$) fits observations well with the use of OPAL opacity. However, as shown in the next section, in our code the evolutionary tracks in the H-R diagram are closer to those of SSMM for $\alpha = 1.5$. Also as described in the next section, the core property, especially the central C/O ratio, is insensitive to this parameter. Therefore, our conclusions are little affected by the choice of a different α . We neither artificially enhance nor suppress convective regions from the Schwarzschild criterion throughout the calculations, and hence we do not include convective overshooting and breathing pulses at the end of He burning. We believe that with the use of the OPAL opacity, these effects will not be so large as once thought (e.g., Stothers & Chin 1991); however, whether these effects are significant or not is still uncertain.

Once the treatment of convection is fixed, the $^{12}\text{C}(\alpha, \gamma)^{16}\text{O}$ rate is the dominant determinant of the C/O ratio after He burning and the C-O core mass size. Since the track in the H-R diagram is not sensitive to the $^{12}\text{C}(\alpha, \gamma)^{16}\text{O}$ rate, it is very difficult to constrain this rate from the surface property of the stars, such as spectral observations of clusters. In this paper this rate is chosen to be 1.5 times the value given by Caughlan & Fowler (1988, CF88 hereafter). With the same treatment for the convection, this choice, denoted by $1.5 \times \text{CF88}$, yields the central carbon mass fraction $X(^{12}\text{C} \simeq 0.20)$ after the He burning of a $25 M_{\odot}$ star (Umeda & Nomoto 1999). Therefore, it approximately reproduces the central C/O ratio of the Nomoto & Hashimoto (1988) model and is expected to be consistent with solar abundances of Ne/O and Mg/O in massive star yield (Hashimoto, Nomoto, & Shigeyama 1989; Thielemann, Nomoto, & Hashimoto 1996; Woosley & Weaver 1995).

TABLE 1
ISOTOPES INCLUDED IN THE NUCLEAR
NETWORK FOR HE BURNING

Isotope	A	Isotope	A
n	1	H	1
He	4	C	12–13
N	13–15	O	14–18
F	17–19	Ne	18–22
Na	21–23	Mg	22–27
Al	25–29	Si	27–30
Fe	56

We note that although the $^{12}\text{C}(\alpha, \gamma)^{16}\text{O}$ rate is constrained most stringently by the nucleosynthesis argument of massive star yield (Weaver & Woosley 1993; Thielemann et al. 1996), our knowledge of this rate is still limited, because there are still uncertainties in the chemical evolution, massive star evolution, and the explosive nuclear burning models. In § 3.3 we examine the dependence of this rate by applying rates of 1.7, 1.5, and 1.0 times the rate of CF88 and the rate of Caughlan et al. (1985, hereafter CF85). More detailed investigation of the C/O ratio in massive stars, its dependence on the $^{12}\text{C}(\alpha, \gamma)^{16}\text{O}$ rate, and treatments of convection will be given in Umeda & Nomoto (1999).

We adopt the solar chemical composition by Anders & Grevesse (1989), the solar He abundance $Y_{\odot} = 0.27753$, and metallicity $Z_{\odot} = 0.02$ (Bahcall & Pinsonneault 1995). We assume that the initial (ZAMS) helium abundance depends on metallicity Z as $Y(Z) = Y_p + (\Delta Y/\Delta Z)Z$ (for $Z \leq 0.02$), where $\Delta Y/\Delta Z$ is a constant and Y_p is the primordial helium abundance. In this paper we adopt $Y_p = 0.247$ (Tytler, Fan, & Burles 1996), and thus $\Delta Y/\Delta Z = 1.5265$. For $Z > 0.02$ we show only the case of $(Z, Y) = (0.03, 0.28)$. Different Y yields different stellar evolution. In particular, the star is brighter when Y is larger. However, as shown below, the effects of changing Y are not very large.

We also include an empirical mass loss rate (de Jager, Nieuwenhuijzen, & van der Hucht 1988) scaled with metallicity as $(Z/0.02)^{0.5}$ (Kudritzki et al. 1989).

3. RESULTS

We calculated the evolution of intermediate-mass (3–9 M_{\odot}) stars for metallicity $Z = 0.001$ – 0.03 . Figure 1 shows the evolution in the H-R diagram and the central density (ρ_c) versus central temperature (T_c) diagram of our 5 M_{\odot} ($Z = 0.02$) model compared with SSMM. The luminosity of

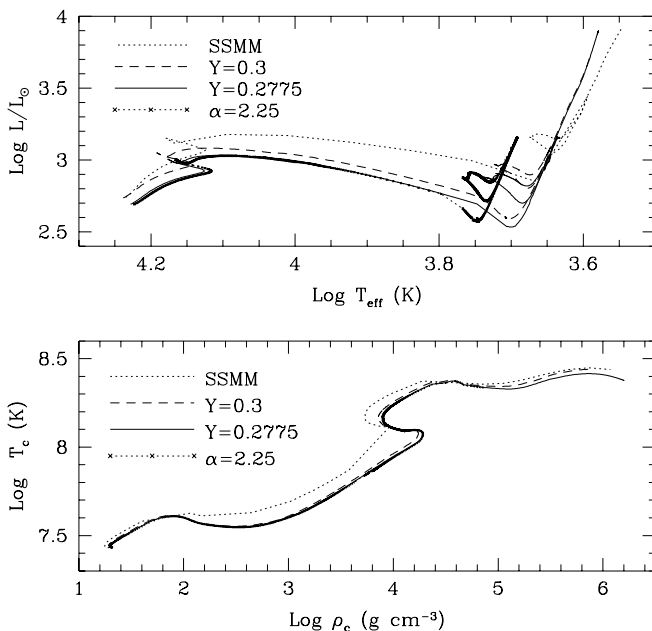


FIG. 1.—Evolution in the H-R diagram (*upper panel*) and the central density (ρ_c) vs. central temperature (T_c) diagram (*lower panel*) of our 5 M_{\odot} ($Z = 0.02$) models for $Y = 0.2775$ (solid line), compared with SSMM (dotted line; Schaller et al. 1992). Dependence on Y is small as, seen from the case of $Y = 0.3$ (dashed line). A model with a larger mixing-length parameter ($\alpha = 2.25$) is shown in a dotted curve with crosses.

our model tends to be lower than that of SSMM, and ρ_c is higher for the same T_c . There are many differences in the inputs, which may be the reason for these differences: we adopt $Y = 0.2775$ for $Z = 0.02$, while SSMM assumed $Y = 0.3$; our choice of the $^{12}\text{C}(\alpha, \gamma)^{16}\text{O}$ rate ($1.5 \times \text{CF88}$) is smaller than $\text{CF85} \sim 2.3 \times \text{CF88}$ used in SSMM; we use a larger nuclear reaction network; and the treatment of convection is different. Most important, they assumed overshooting from a convective core, which we do not. Figure 1 shows that the difference of Y alone does not explain the discrepancy. Also, we find that the tracks on the H-R diagrams are almost identical even though the $^{12}\text{C}(\alpha, \gamma)^{16}\text{O}$ rate is different. Therefore, it is probably the treatment of convection that is mainly responsible for the differences. Indeed, the tracks on the H-R diagrams of the no-overshooting models in Bressan et al. (1993) are similar to our results.

In this figure we also show the effect of mixing-length parameter α for the outermost superadiabatic convection. This parameter changes location in the H-R diagram after a star becomes a red giant. On the other hand, the central ρ_c – T_c track is almost independent of this parameter. As a result, the central C/O ratio is almost identical in the $\alpha = 1.5$ and $\alpha = 2.25$ cases. Therefore, the choice of this parameter is not so important for the purposes of this paper. Chieffi et al. (1995) found that $\alpha = 2.25$ fits observations well; however, the evolutionary tracks in the H-R diagram are closer to those of SSMM for $\alpha = 1.5$ than for $\alpha = 2.25$, and hence we adopt $\alpha = 1.5$ in the following.

3.1. Metallicity Effects on Stellar Evolution

In the ranges of stellar masses and Z considered in this paper, the most important metallicity effect is that the radiative opacity is smaller for lower Z . Therefore, a star with lower Z is brighter, and thus has a shorter lifetime than a star with the same mass but higher Z . In this sense, the effect of reducing metallicity for these stars is almost equivalent to increasing a stellar mass. This is verified in Figure 2, which shows H-R diagrams of 5 M_{\odot} models with different metallicities (*upper panel*) and models with $Z = 0.02$ for different stellar masses (*lower panel*).

For stars with larger masses and/or smaller Z , the luminosity is higher at the same evolutionary phase. With a higher nuclear energy generation rate, these stars have larger convective cores during H and He burning, thus forming larger He and C-O cores. This property is depicted in Figures 3a and 3b.

Figure 3a shows abundances in mass fraction in the inner core of a 7 M_{\odot} star for $Z = 0.001$ at age $t = 48.45$ Myr, with the central temperature and density $\text{log } T_c [\text{K}] = 8.58$ and $\text{log } \rho_c [\text{g cm}^{-3}] = 6.82$. In Figure 3a, the He burning shell is located around the mass coordinate $M_r = 1.1 M_{\odot}$, which indicates that the C-O core of this model will exceed 1.1 M_{\odot} . Since this is well above the critical mass for the off-center carbon ignition, this star will ignite carbon in the nondegenerate region and will not form a C-O WD but rather an O-Ne-Mg core (Nomoto 1984).

If a star is less massive or has higher metal abundance than the model in Figure 3a, the C-O core can be smaller and carbon ignition is avoided, as shown in Figure 3b for the 7 M_{\odot} model of $Z = 0.02$ at age $t = 51.87$ Myr (at the end of the second dredge-up). The dredge-up is a phenomenon during which the surface convection penetrates inward and inner material is brought to the surface. For

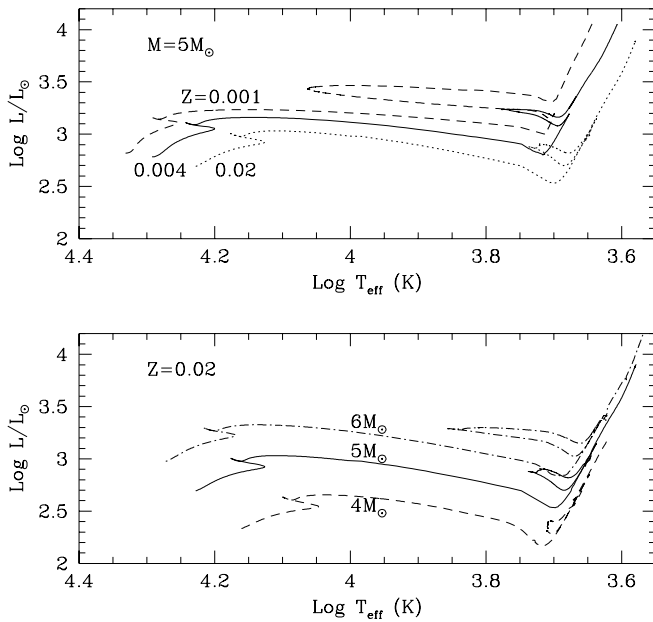


FIG. 2.—Evolution in the H-R diagrams of the $5 M_{\odot}$ models for several metallicities Z (upper panel) and the $Z = 0.02$ models for several stellar masses (lower panel).

intermediate-mass stars, the first dredge-up occurs before or around the He ignition and the second during the He shell burning stage. During the second dredge-up phase, the thick He shell seen in Figure 3a becomes progressively thinner because of the growth of the C-O core growth resulting from He shell burning and the penetration of the surface convection. Therefore, as shown in Figure 3b, the He shell becomes very thin (in mass coordinate) at the end

of the second dredge-up phase. Chemical abundances at the end of the second dredge-up for the 6 and $4 M_{\odot}$ stars (with $Z = 0.02$) are shown in Figures 4 and 5, respectively.

3.2. ZAMS Mass Ranges of SN Ia Progenitors

Stars that do not ignite carbon will evolve into the asymptotic giant branch (AGB) phase. During this phase, if they are single stars, the C-O core mass increases slightly, because of H-He double shell burning, until they lose almost all hydrogen-rich envelopes by wind mass loss. If they are in close binary systems, their hydrogen-rich envelopes are stripped off much more quickly, owing to the Roche lobe overflow, and C-O WDs are left. When the companion star evolves off the main-sequence, mass transfer occurs from the companion star to the WD. A certain class of these accreting WDs become SNe Ia, depending on the accretion rate and the initial mass of the WD (e.g., Nomoto 1982; Nomoto & Kondo 1991)

The WD mass at the onset of mass transfer from the companion star (denoted by $M_{\text{WD},0}$) is critically important for the fate of the accreting WD. For $M_{\text{WD},0}$ as low as $\lesssim 0.7 M_{\odot}$, it is difficult for the WD mass to reach $M_{\text{Ia}} \approx 1.37\text{--}1.38 M_{\odot}$. For higher $M_{\text{WD},0}$, the WD can become a SNe Ia in a some binary systems (Hachisu, Kato, & Nomoto 1996; Li & van den Heuvel 1996). However, the $M_{\text{WD},0}$ depends on various uncertain factors, such as binary separation, the effects of recurring He shell flashes, and mass loss rate during the AGB phase. In the following discussion, we assume that $M_{\text{WD},0}$ is not significantly larger than the C-O core mass at the end of the second dredge-up phase, which we denote M_{CO} .

Figure 6 shows the metallicity dependence of the relation between the ZAMS mass (M_{ms}) and M_{CO} . We note that

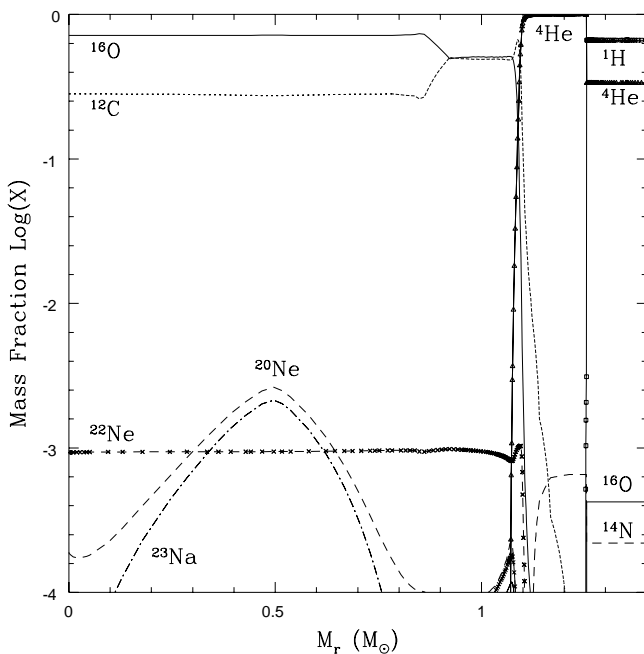


FIG. 3a

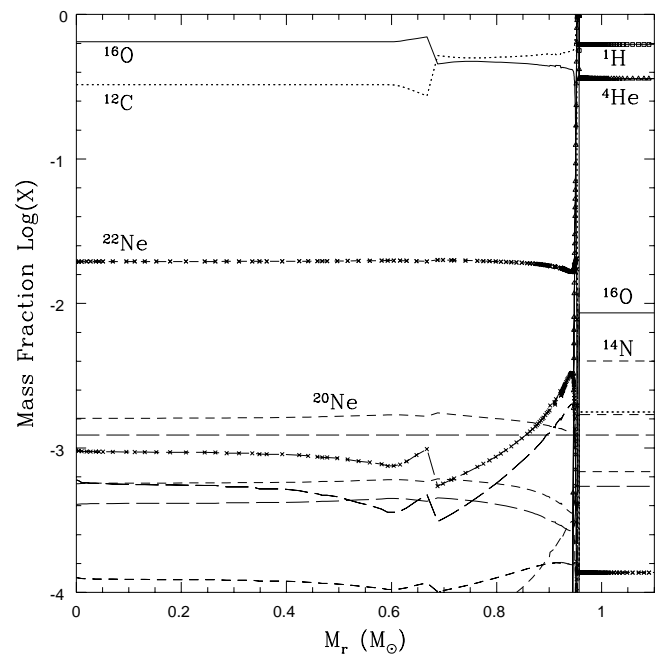


FIG. 3b

FIG. 3.—(a) Abundances in mass fraction in the inner core of the $7 M_{\odot}$ star for $Z = 0.001$ at age $t = 48.45$ Myr, with the central temperature and density $\log T_c(\text{K}) = 8.58$ and $\log \rho_c(\text{g cm}^{-3}) = 6.82$. The maximum temperature, $\log T_{\text{max}} = 8.78$, is attained at $M_r = 0.54 M_{\odot}$. (b) Same as Fig. 3a, but for $Z = 0.02$ at the end of the second dredge-up and $t = 51.87$ Myr, with $\log T_c = 8.29$ and $\log \rho_c = 7.04$. Maximum temperature, $\log T_{\text{max}} = 8.69$, is attained at $M_r = 0.72 M_{\odot}$.

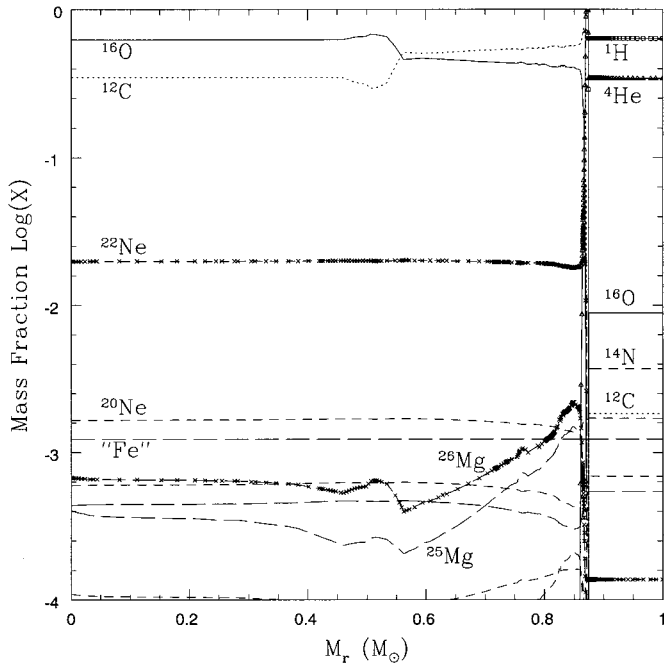


FIG. 4.—Same as Fig. 3b, but for $M = 6 M_{\odot}$

stars with higher metallicity form smaller C-O cores if they have the same M_{ms} . Our M_{ms} versus M_{CO} relations are similar to those of Castellani et al. (1990), who used the Los Alamos opacity (Huebner et al. 1977) and assumed overshooting but suppressed breathing pulses at the end of He burning. They calculated $Z = 0.02, 0.006,$ and 0.002 cases and $Y = 0.23$ and 0.27 cases for 3, 4, 5, 7, and 9 M_{\odot} stars. Our M_{ms} versus M_{CO} relations are also consistent with those of Vassiliadis & Wood (1993), who used OPAL opacity without overshooting.

Figure 7 shows M_{UP} as a function of metallicity, which is compared with BI79 and CCPT. Our results in these figures

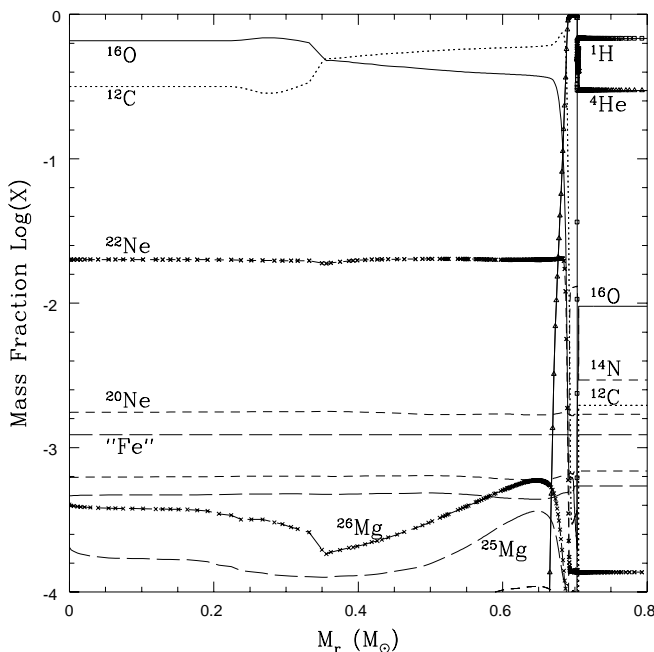


FIG. 5.—Same as Fig. 3b, but for $M = 4 M_{\odot}$

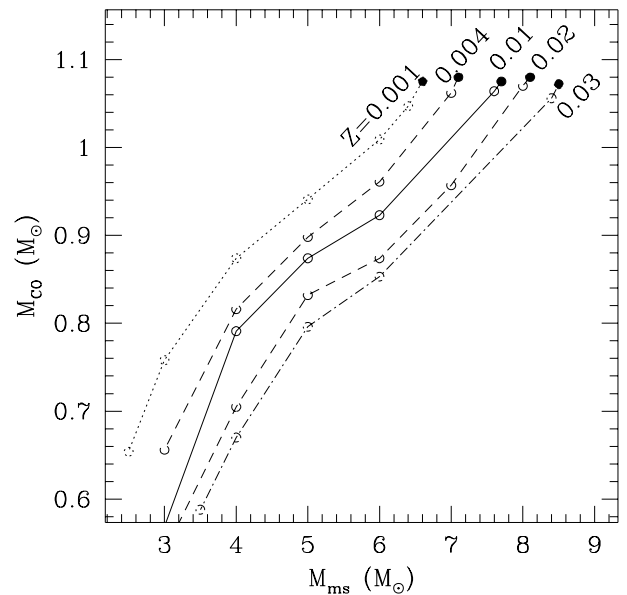


FIG. 6.—Metallicity dependence of the ZAMS mass (M_{ms}) vs. C-O core mass (M_{CO}) at the end of the second dredge-up. Filled circles indicate that off-center carbon ignition occurs in these models. Hence, the abscissa of these points correspond to the M_{UP} .

are quantitatively different from BI79, because BI79 used the old Cox & Stewart (1970) opacity. Our results are also different from CCPT's because they assumed relatively large overshooting.

Although Castellani et al. (1990) did not estimate M_{UP} exactly, their results indicate that their M_{UP} lies closer to ours than to those of BI79 and CCPT. CCPT and Castellani et al. (1990) assumed strong overshooting, but we note that when OPAL opacity is used, the overshooting effect should not be very large if it is to meet the observational constraints (Stothers & Chin 1991). Schaerer et al. (1993)

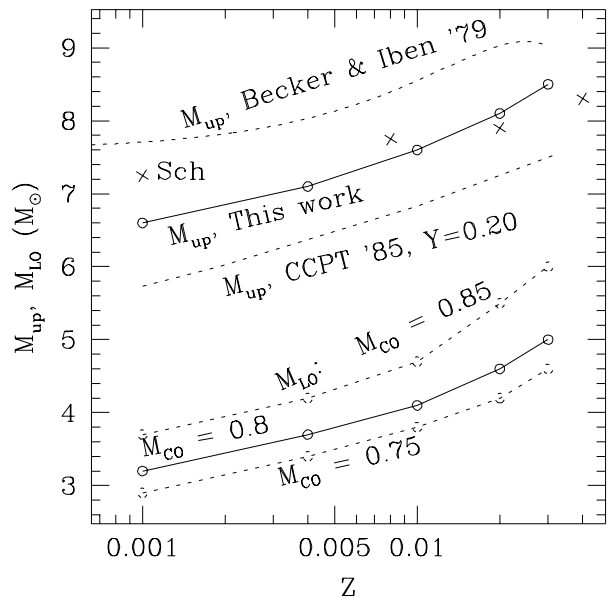


FIG. 7.— M_{UP} obtained in this work compared with earlier works. The lower ZAMS mass limit for becoming an SN Ia, M_{LO} , is also shown. Since this value depends on the binary parameters, three curves are shown, which correspond to $M_{CO} = 0.75, 0.80,$ and $0.85 M_{\odot}$. Crosses labeled by "Sch" are M_{UP} of Schaerer et al. (1993).

also estimated M_{UP} by comparing their grids of stellar models with T_c versus ρ_c tracks in Maeder & Meynet (1989), which is shown in Figure 7 by the crosses. Our results show a stronger metallicity dependence than do those of Schaerer et al. (1993). In particular, their M_{UP} at $Z = 0.001$ is significantly larger than ours.

Tornambè & Chieffi (1986) studied M_{UP} for very extremely metal-deficient stars ($Z \leq 10^{-4}$) and found that the M_{UP} increases for smaller Z . Though verifying this result may be interesting, we do not treat these extremely low-metal stars, because stars with $Z < 10^{-3}$ cannot become SNe Ia progenitors in the Chandrasekhar mass model (Kobayashi et al. 1998).

In Figure 7 we also plot M_{LO} , which is defined as the lower ZAMS mass limit for stars to become SNe Ia. Here we assume that in order for the accreting WD to reach M_{Ia} , M_{CO} should be larger than a certain critical mass, typically $\sim 0.8 M_{\odot}$ (Hachisu et al. 1996). Since this critical M_{CO} depends on the binary parameters, three cases of M_{CO} are shown in Figure 7.

In Figure 8 we show the number of SNe Ia progenitors, i.e., the number of stars in the range $M_{LO} \leq M \leq M_{UP}$, normalized to the case of $Z = 0.02$ and $M_{CO} = 0.8 M_{\odot}$. Since the value of M_{LO} is sensitive to M_{CO} , which depends on the binary parameters, we consider four cases of M_{LO} in Figure 8. The Salpeter initial mass function (IMF) is used to obtain this figure. The figure shows that if Salpeter IMF holds also in a lower metallicity environment, the number of SNe Ia progenitors increases toward low metallicity, because stars with lower metallicity have larger C-O cores for the same M_{ms} . It should be noted that these numbers are not necessarily proportional to the SNe Ia rate, because in order to calculate this rate the binary companion's lifetime must be taken into account.

3.3. C/O Ratio in White Dwarfs

From Figures 3–5, we find that the central part of these stars is oxygen-rich. The C/O ratio is nearly constant in the

innermost region, which was a convective core during He burning. Outside this homogeneous region, where the C-O layer grows owing to He shell burning, the C/O ratio increases up to $C/O \gtrsim 1$; thus the oxygen-rich core is surrounded by a shell with $C/O \gtrsim 1$. In fact, this is a generic feature in all the models that we calculated. The C/O ratio in the shell is $C/O \simeq 1$ for stars as massive as $\sim 7 M_{\odot}$ (Fig. 3b) and $C/O > 1$ for less massive stars (Figs. 4 and 5).

In most cases of our calculations as well as previous ones, from the center to the C-O core edge, the oxygen abundance has a peak near the outer edge of the oxygen-rich core. This configuration is Rayleigh-Taylor unstable and will be rehomogenized by convection (Salaris et al. 1997). Their results show that the rehomogenization proceeds slowly, and the effect is relatively small during the liquid phase of the WD interior. However, because of this effect, the final chemical profile of the inner SNe Ia progenitors may differ from the profile at the end of second dredge-up, depending on the timescale of its becoming a SNe Ia.

Figure 9 shows the central C/O ratio in mass fraction, which is not a monotonic function of the metallicity and the ZAMS mass. One reason for this complexity is that the C/O ratio is sensitive to evolutionary change in the convective core size during the later stage of He burning. Small differences in the core temperature and opacity lead to a different evolutionary behavior of the convective core, which largely changes the C/O ratio.

The central C/O ratio is sensitive to the $^{12}\text{C}(\alpha, \gamma)^{16}\text{O}$ rate. For example, for $M = 5 M_{\odot}$, $Z = 0.02$, and $Y = 0.27753$, this ratio is 0.58 for the CF88 $\times 1.5$ rate, while $C/O = 0.89$, 0.47, and 0.24 for the CF88, CF88 $\times 1.7$, and CF85 rates, respectively. This ratio, on the other hand, is not so sensitive to Y : for example, $C/O = 0.58$ and 0.53 for $Y = 0.285$ and $Y = 0.30$, respectively. Several groups, including Salaris et al. (1997) and Bressan et al. (1993), calculated the central C and O mass fractions for solar metallicity. SSMM and a series of subsequent papers calculated the fractions for various metallicities. Our results of the central C/O ratio is

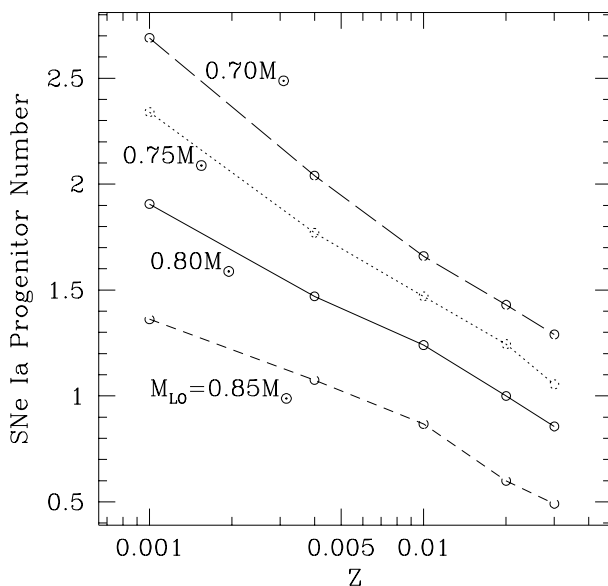


FIG. 8.—Metallicity and M_{LO} dependence of the number of SNe Ia progenitors normalized to the case with $Z = 0.02$ and $M_{LO} = 0.8 M_{\odot}$. The Salpeter IMF is assumed.

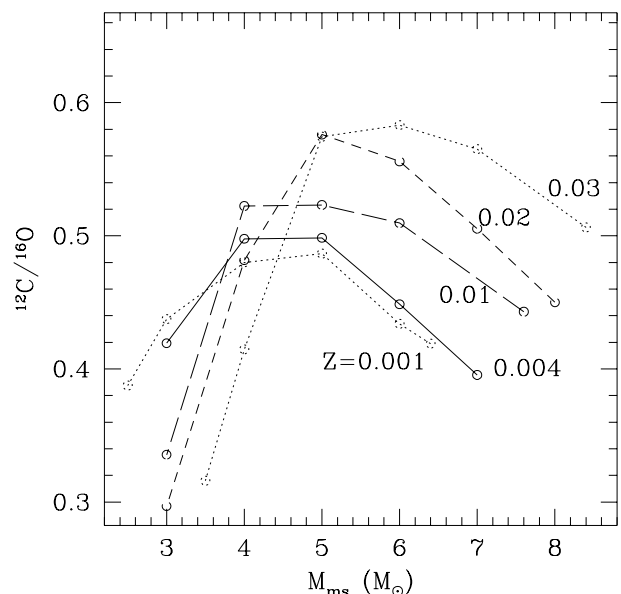


FIG. 9.—Central C/O ratio in mass fraction as a function of metallicity and stellar mass.

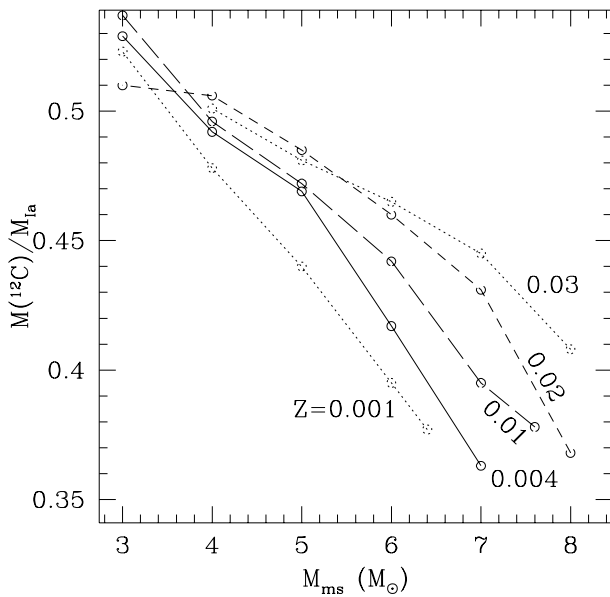


FIG. 10.—Total ^{12}C mass [$M(^{12}\text{C})$] included in the WD of mass $M_{\text{Ia}} = 1.37 M_{\odot}$ just before an SN Ia explosion as a function of M_{ms} .

systematically larger than those of SSMM and Salaris et al. (1997), who adopted the CF85 $^{12}\text{C}(\alpha, \gamma)^{16}\text{O}$ rate and different treatments of convection.

Figure 10 shows the total mass of ^{12}C [$M(^{12}\text{C})$] integrated over the WD mass, $M_{\text{Ia}} \simeq 1.37 M_{\odot}$, just before the SN Ia explosion. Here we assume $\text{C/O} \sim 1$ in the outer layer of $M_{\text{CO}} \leq M_r \leq M_{\text{Ia}}$, which is formed by He shell burning during accretion. This is because our results as well as other previous works indicate that a star with C–O core mass heavier than $\sim 1 M_{\odot}$ tends to yield $\text{C/O} \sim 1$ in the product of He shell burning. We note that C/O depends on both the (ρ, T) track and the nuclear reaction rate. For

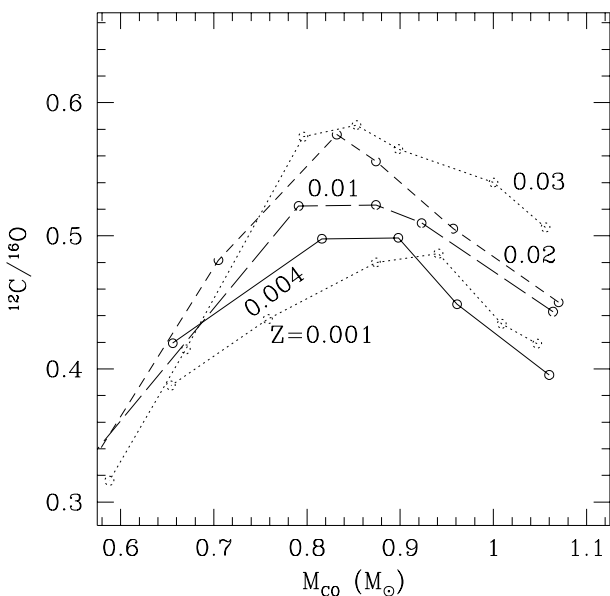


FIG. 11.—Central C/O ratio in mass fraction as a function of metallicity and M_{CO} .

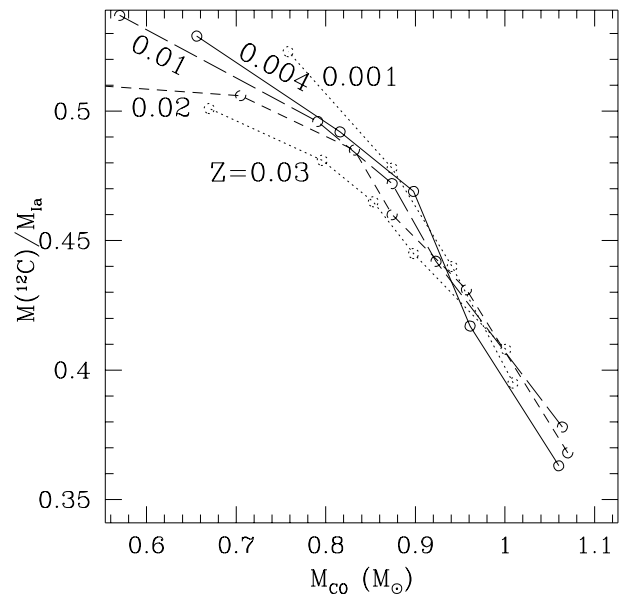


FIG. 12.—Total ^{12}C mass [$M(^{12}\text{C})$] included in the WD of mass $M_{\text{Ia}} = 1.37 M_{\odot}$ just before an SN Ia explosion as a function of M_{CO} .

example, if we use CF88 for the $^{12}\text{C}(\alpha, \gamma)^{16}\text{O}$ rate in the model of Figure 3b, the C/O ratio in the shell is $\text{C/O} \simeq 1.46$.

The total carbon mass is important for studying SNe Ia, because it determines the total explosion energy. The total carbon mass fraction, $M(^{12}\text{C})/M_{\text{Ia}}$, varies in the range of 0.36–0.5, depending on the ZAMS mass and metallicity, which might be related to the observed variation of the SNe Ia brightness.

In Figures 11 and 12 we plot the central C/O ratio and $M(^{12}\text{C})$ again, but the abscissa is changed to M_{CO} . These figures show that by changing the abscissa from M_{ms} to M_{CO} , these curves somewhat converge. The implication of this is discussed in the next section.

4. SUMMARY AND DISCUSSION

We have calculated stellar evolution through the carbon ignition or the second dredge-up for $M = 3$ – $9 M_{\odot}$ and $Z = 0.001$ – 0.03 . Using these evolutionary models, we have made systematic investigations of the stellar metallicity and mass dependencies of the C–O core mass M_{CO} at the end of the second dredge-up, the C/O ratio in the C–O core, and the mass range $(M_{\text{LO}}, M_{\text{UP}})$. The major effect of changing metallicity appears in the M_{CO} – M_{ms} relation (Figs. 9 and 11). Our main conclusions and the implications for SNe Ia are as follows:

1. The Z dependences of M_{UP} and M_{LO} are important for obtaining the white dwarf luminosity function and for modeling galactic chemical evolution, because these determine the SNe Ia rate. Our results show that both M_{UP} and M_{LO} are smaller for lower Z . This implies that if the initial mass function is independent of metallicity, the number density of SN Ia progenitors is larger in a lower metallicity environment (Fig. 8); therefore, the luminosity function of WDs and SNe Ia would depend on Z .

2. Our results indicate that the innermost part of C–O WDs is likely to be oxygen-rich ($\text{C/O} \lesssim 0.6$) rather than $\text{C/O} = 1$, as is usually assumed in the SNe Ia modeling. We find two tendencies for the central C/O ratio: (1) For a fixed

Z , as stellar mass increases, the C/O ratio at the stellar center first increases to the maximum and then decreases. Peaks, which depend on metallicity, are seen at lower mass in our results ($M_{\text{ms}} \sim 5 M_{\odot}$) than in SSMM ($M_{\text{ms}} \sim 7 M_{\odot}$). (2) For larger Z , the above maximum C/O ratio is larger. Compared with SSMM, our results show a much larger variation in the C/O ratio distribution.

3. For WDs that can be progenitors of SNe Ia, the central ratio varies in the range of $C/O = 0.4\text{--}0.6$, depending mainly on the ZAMS mass. The total carbon mass fraction just before SN Ia explosion is found to vary in the range $M(^{12}\text{C})/M_{\text{Ia}} = 0.36\text{--}0.5$. These may be partially responsible for the observed variations in the brightness and spectra of SNe Ia.

Most previous works on SNe Ia explosion have used progenitor models with $C/O = 1$. Only recently Höflich et al. (1998) have started calculations with different C/O for the DD models. The variation of C/O ratio would be important, because as the inner regions are burned during the deflagration phase, the energy release is changed and, consequently, the pre-expansion of the outer layers is modified. This changes the total explosion energy, and hence the expansion rate of the SNe Ia and the brightness and shape of light curves as well. It may also affect the ρ_{tr} in the DD model to induce a large variation in the explosion energy.

4. The ranges of the variation in the central C/O ratio and $M(^{12}\text{C})/M_{\text{Ia}}$ obtained above do not significantly depend on Z for $0.001 \leq Z \leq 0.02$. These ratios, shown in Figures 9 and 10, exhibit smaller dispersion with respect to metallicity if they are plotted against M_{CO} (Figs. 11 and 12). We conclude that the metallicity effects are relatively minor for the same M_{CO} , although there are still some significant variations in the central C/O ratio for $M_{\text{CO}} \gtrsim 0.8 M_{\odot}$ (Fig. 11). Moreover, WDs with $Z \lesssim 0.002$ need not be considered as SNe Ia progenitors, because the winds of such low-metallicity WDs are too weak for them to evolve into SNe Ia (Kobayashi et al. 1998). These would be good for determining cosmological parameters with the use of SNe Ia, because “evolutionary” effects on the SN Ia properties are minor at different red shifts.

We thank H. Saio for kindly providing us his code, and P. Höflich, N. Prantzos, and F.-K. Thielemann for useful conversation. This work has been supported in part by grants-in-aid for scientific research (05242102, 06233101, 6728, 10147212) and COE research (07CE2002) of the Ministry of Education, Science and Culture in Japan, and by the National Science Foundation under grant PHY94-07194.

REFERENCES

- Anders, E., & Grevesse, N. 1989, *Geochim. Cosmochim. Acta*, 53, 197
 Bahcall, J. N., & Pinsonneault, M. H. 1995, *Rev. Mod. Phys.*, 67, 781
 Becker, S. A., & Iben, I. 1979, *ApJ*, 232, 831 (B179)
 Branch, D., Romanishin, W., & Baron, E. 1996, *ApJ*, 465, 73
 Branch, D., & Tammann, G. A. 1992, *ARA&A*, 30, 359
 Bressan, A., Fagotto, F., Bertelli, G., & Chiosi, C. 1993, *A&AS*, 100, 647
 Castellani, V., Chieffi, A., Pulone, L., & Tornambè, A. 1985, *ApJ*, 294, L31 (CCPT)
 Castellani, V., Chieffi, A., & Straniero, O. 1990, *ApJS*, 74, 463
 Caughlan, G., & Fowler, W. 1988, *Atomic Data Nucl. Data Tables*, 40, 283 (CF88)
 Caughlan, G., Fowler, W., Harris, M. J., & Zimmermann, B. A. 1985, *Atomic Data Nucl. Data Tables*, 32, 197 (CF85)
 Charbonnel, C., Meynet, G., Maeder, A., Schaller, G., & Schaerer, D. 1993, *A&AS*, 101, 415
 Chieffi, A., Straniero, O., & Salaris, M. 1995, *ApJ*, 445, L39
 Cox, A. N., & Stewart, J. N. 1970, *ApJS*, 19, 243
 de Jager, C., Nieuwenhuijzen, H., & van der Hucht, K. 1988, *A&AS*, 72, 259
 Hachisu, I., Kato, M., & Nomoto, K. 1996, *ApJ*, 470, L97
 Hamuy, M., Phillips, M. M., Schommer, R. A., & Suntzeff, N. B. 1996, *AJ*, 112, 2391
 Hashimoto, M., Nomoto, K., & Shigeyama, T. 1989, *A&A*, 210, L5
 Höflich, P., & Khokhlov, A. 1996, *ApJ*, 457, 500
 Höflich, P., Wheeler, J. C., & Thielemann, F.-K. 1998, *ApJ*, 495, 617
 Huebner, W. F., Merts, A. L., Magee, N. H., & Argo, M. F. 1977, *Los Alamos Sci. Lab. Rep.*, LA-670-M
 Iglesias, C. A., & Rogers, F. F. 1993, *ApJ*, 412, 752
 Itoh, N., Nishikawa, A., & Kohyama, Y. 1996, *ApJS*, 102, 411
 Khokhlov, A. 1991, *A&A*, 245, 114
 Kobayashi, C., Tsujimoto, T., Nomoto, K., Hachisu, I., & Kato, M. 1998, *ApJ*, 503, L155
 Kudritzki, R., Pauldrach, A., Puls, J., & Abbott, D. 1989, *A&A*, 219, 205
 Li, X.-D., & van den Heuvel, E. P. J. 1997, *A&A*, 322, L9
 Maeder, A., & Meynet, G. 1989, *A&A*, 210, 155
 Mazzitelli, I., & D’Antona, F. 1986a, *ApJ*, 308, 706
 ———. 1986b, *ApJ*, 311, 762
 Nomoto, K. 1982, *ApJ*, 253, 798
 ———. 1984, *ApJ*, 277, 791
 Nomoto, K., & Hashimoto, M. 1988, *Phys. Rep.*, 163, 13 (NH88)
 Nomoto, K., Iwamoto, K., & Kishimoto, N. 1997, *Science*, 276, 1378
 Nomoto, K., & Kondo, Y. 1991, *ApJ*, 367, L19
 Nomoto, K., Sugimoto, D., & Neo, S. 1976, *Ap&SS*, 39, L37
 Nomoto, K., Thielemann, F.-K., & Yokoi, K. 1984, *ApJ*, 286, 644
 Phillips, M. M. 1993, *ApJ*, 413, L75
 Ruiz-Lapuente, P., Canal, R., & Isern, J., ed. 1997, *Thermonuclear Supernovae* (Dordrecht: Kluwer)
 Saio, H., & Nomoto, K. 1998, in *Computational Astrophysics: Stellar Physics*, ed. R. Kudritzki, D. Mihalas, K. Nomoto, & F.-K. Thielemann (New York: Springer), in press
 Salaris, M., Dominguez, I., Garcia-Berro, E., Hernanz, M., Isern, J., & Mochkovitch, R. 1997, *ApJ*, 486, 413
 Sandage, A., & Tammann, G. A. 1993, *ApJ*, 415, 1
 Schaerer, D., Charbonnel, C., Meynet, G., Maeder, A., & Schaller, G. 1993, *A&AS*, 102, 339
 Schaller, G., Schaerer, D., Meynet, G., & Maeder, A. 1992, *A&AS*, 96, 269 (SSMM)
 Spruit, H. C. 1992, *A&A*, 253, 131
 Stothers, R. B., & Chin, C.-W. 1991, *ApJ*, 381, L67
 Thielemann, F.-K., Nomoto, K., & Hashimoto, M. 1996, *ApJ*, 460, 408
 Tornambè, A., & Chieffi, A. 1986, *MNRAS*, 220, 529
 Tytler, D., Fan, X.-M., & Burles, S. 1996, *Nature*, 381, 207
 Umeda, H., & Nomoto, K. 1999, in preparation
 Vassiliadis, E., & Wood, P. R. 1993, *ApJ*, 413, 641
 Weaver, T. A., & Woosley, S. E. 1993, *Phys. Rep.*, 227, 665
 Woosley, S. E., & Weaver, T. A. 1994, in *Supernovae*, Les Houches Session LIX, ed. S. A. Bludman, R. Mochkovitch, & J. Zinn-Justin (Amsterdam: Elsevier), 63
 Woosley, S. E., & Weaver, T. A. 1995, *ApJS*, 101, 181
 Yamaoka, H., Nomoto, K., Shigeyama, T., & Thielemann, F.-K. 1992, *ApJ*, 393, 55